*Supporting Information for*

# Colloidal Bismuth Nanocrystals as a Model Anode Material for Rechargeable Mg-Ion Batteries: Atomistic and Mesoscale Insights

*Kostiantyn V. Kravchyk,* [1,2] *Laura Piveteau,* [1,2] *Riccarda Caputo,* [1**] *Meng He,* [1,2] *Nicholas P. Stadie,* [1,2***] *Maryna I. Bodnarchuk,* [2] *Rainer T. Lechner,* [3] *and Maksym V. Kovalenko*[1,2*]

[1]Department of Chemistry and Applied Biosciences, ETH Zürich, Vladimir-Prelog-Weg 1, Zurich, CH-8093, Switzerland.

[2]Empa-Swiss Federal Laboratories for Materials Science and Technology, Überlandstrasse 129, Dübendorf, CH-8600, Switzerland.

[3]Institute of Physics, Montanuniversitaet Leoben, Franz-Josef-Strasse 18, A-8700 Leoben, Austria.

[*]Email: mvkovalenko@ethz.ch.

[**]Current address: ICQMS, International Centre for Quantum and Molecular Structures, Department of Physics, Shanghai University, China.

[***]Current address: Department of Chemistry and Biochemistry, Montana State University, Bozeman, Montana, 59717, USA.

KEYWORDS: mg-ion battery, magnesium, energy storage, nanocrystal, synthesis.

**Table S1**. Lattice parameters of Mg, Bi, and the trigonal and cubic phases of $Mg_3Bi_2$ calculated using different functionals. The lattice parameters, in Å, and the fractional atomic positions are reported in the hexagonal lattice representation for Bi and α-$Mg_3Bi_2$, for which the lattice angles are 90, 90, and 120 degrees.

| **Species** | **Functional** | **Lattice Parameter a, c (Å)** | **Atomic Positions** | **Reference Lattice Parameter a, c (Å)** |
|---|---|---|---|---|
| **Mg** *$P6_3/mmc$* (IT No 194) | GGA-PBE | 3.338, 5.484 | 1/3, 2/3, 1/4 | 3.22, 5.23 [1] |
| | GGA-PBE-D | 3.215, 5.278 | | |
| | LDA-CA-PZ | 3.267, 5.368 | | |
| | LDA-CA-PZ-OBS | 3.215, 5.283 | | |
| **Bi** *R-3m* (IT No 166) | GGA-PBE | 4.498, 11.666 | 0, 0, 0.2352 | 4.535, 11.814 [2] |
| | LDA-CA-PZ | 4.400, 11.088 | 0, 0, 0.2387 | |
| | LDA-CA-PZ-D | 4.391, 11.040 | 0, 0, 0.2391 | |
| **α-$Mg_3Bi_2$** *$P\text{-}3m_1$* (IT No 164) | GGA-PBE | 4.784, 7.513 | Mg (1a) 0, 0, 0, | 4.666, 7.401 [3] |
| | | | Mg (2d) 1/3, 2/3, 0.6295 | |
| | | | Bi (2d) 1/3, 2/3, 0.2204 | |
| | GGA-PW91 | 4.771, 7.522 | Mg (1a) 0, 0, 0 | |
| | | | Mg (2d) 1/3, 2/3, 0.6259 | |
| | | | Bi (2d) 1/3, 2/3, 0.2213 | |
| | **LDA-CA_PZ** | **4.667, 7.323** | Mg (1a) 0, 0, 0 | |
| | | | Mg (2d) 1/3, 2/3, 0.6305 | |
| | | | Bi (2d) 1/3, 2/3, 0.2192 | |
| | LDA-CA-PZ-D | 4.627, 7.255 | Mg (1a) 0, 0, 0 | |
| | | | Mg (2d) 1/3, 2/3, 0.6301 | |
| | | | Bi (2d) 1/3, 2/3, 0.2177 | |
| **β-$Mg_3Bi_2$** *Ia-3* (IT No 206) | **LDA-CA_PZ** | 13.611 | Mg (48e) 0.1099, 0.3665, 0.1276 | none |
| | | | Bi (8a) 0, 0, 0 | |
| | | | Bi (24d) 0.2667, 0, 1/4 | |

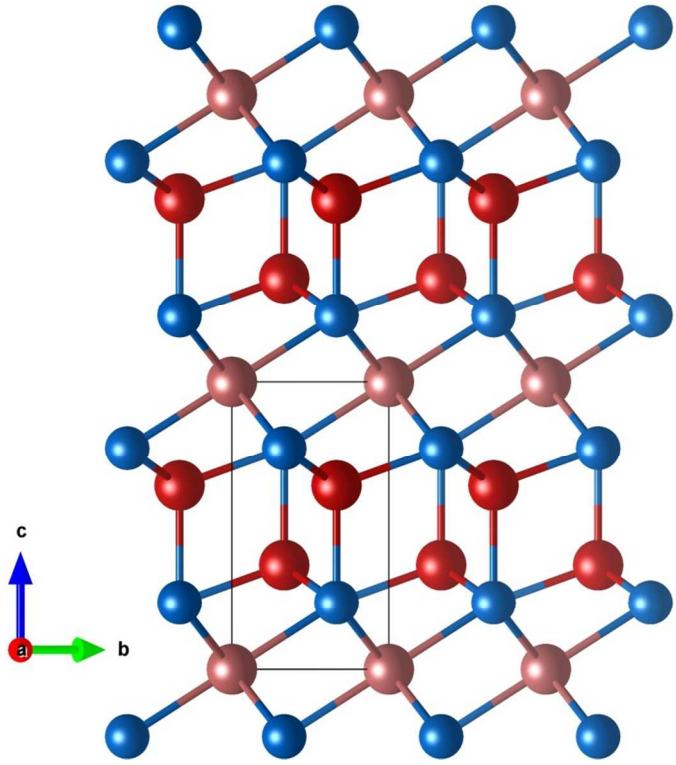


**Figure S1**. α-$Mg_3Bi_2$ structure, viewed along the crystallographic *a* axis. The Mg atoms in the octahedral sites are represented in bronze and those in the tetrahedral sites in red.

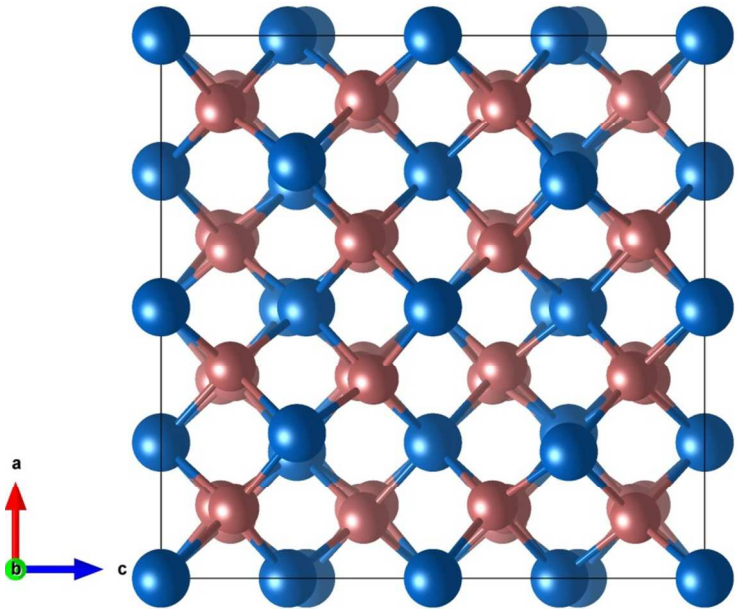


**Figure S2.** A view of β-$Mg_3Bi_2$ structure along the crystallographic *b* axis. The Mg atoms, equivalent by symmetry, are located in the tetrahedral sites and shown in bronze. The shortest Mg-Mg distance is along the crystallographic **a**-direction, with a value of 3.587 Å.

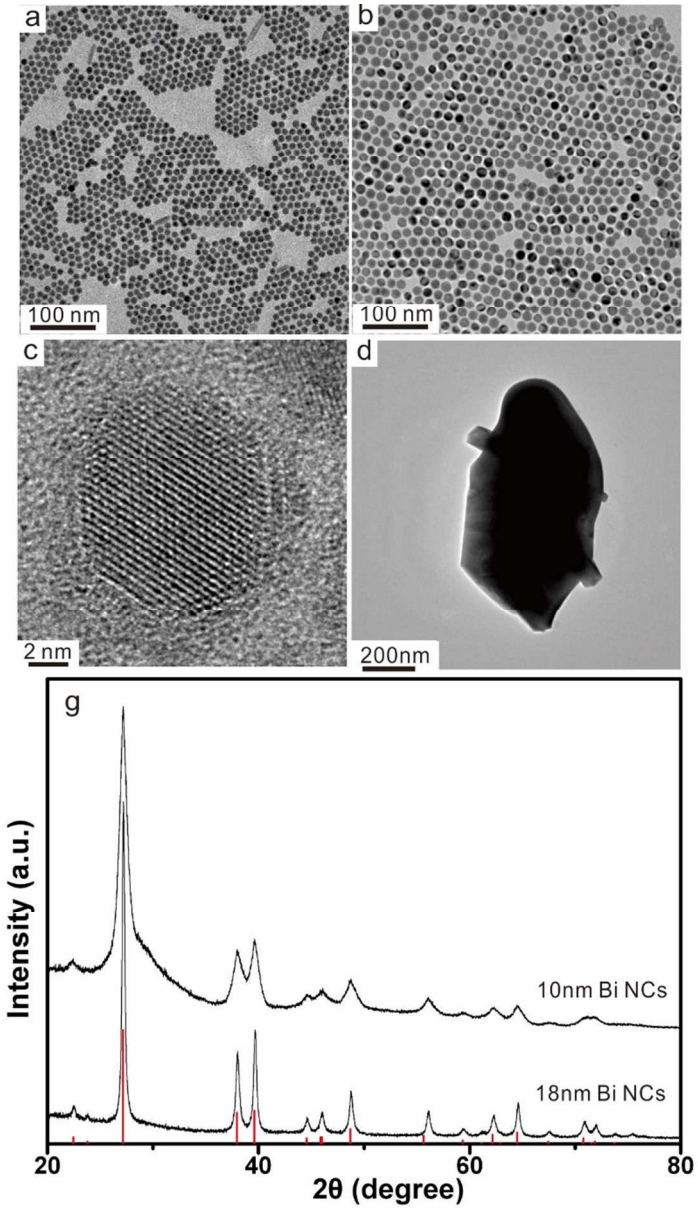


**Figure S3.** TEM images of (a) 10 nm and (b) 18 nm Bi NCs; (c) HR-TEM image of a 10 nm Bi NC; (d) TEM image of a crystallite of the microcrystalline bulk Bi; (g) powder XRD patterns of 10 nm and 18 nm Bi NCs. Red vertical lines mark the reflections from the bulk Bi.

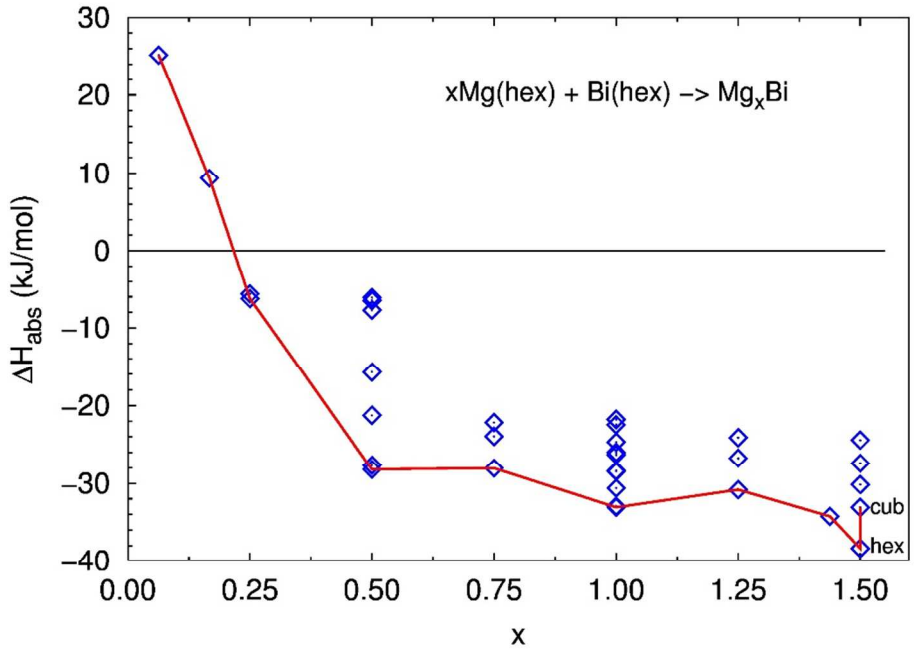


**Figure S4**. The calculated enthalpy of absorption of Mg in Bi, expressed in kJ/mol of Mg. The reference states are the elemental solid state structures of Mg and Bi. The red line indicates the lowest energy structures at each composition.

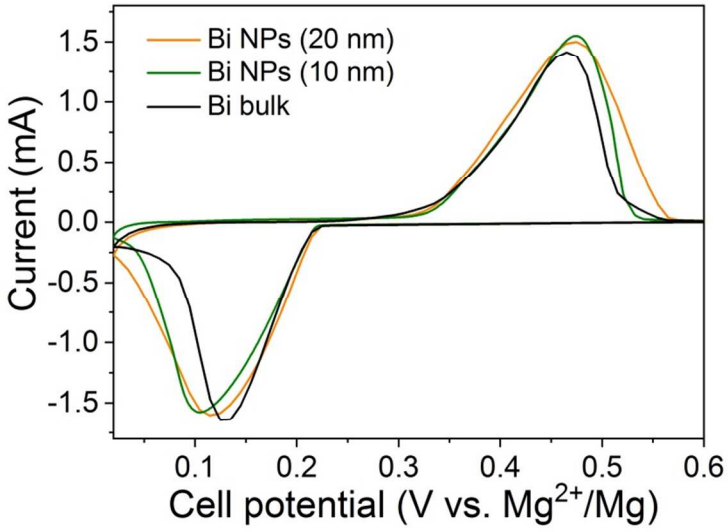


**Figure S5.** Cyclic voltammograms for 10 nm Bi NCs, 18 nm Bi NCs and bulk Bi measured at scan speed of 0.1 mV $s^{-1}$ during the 10$^{th}$ cycle.

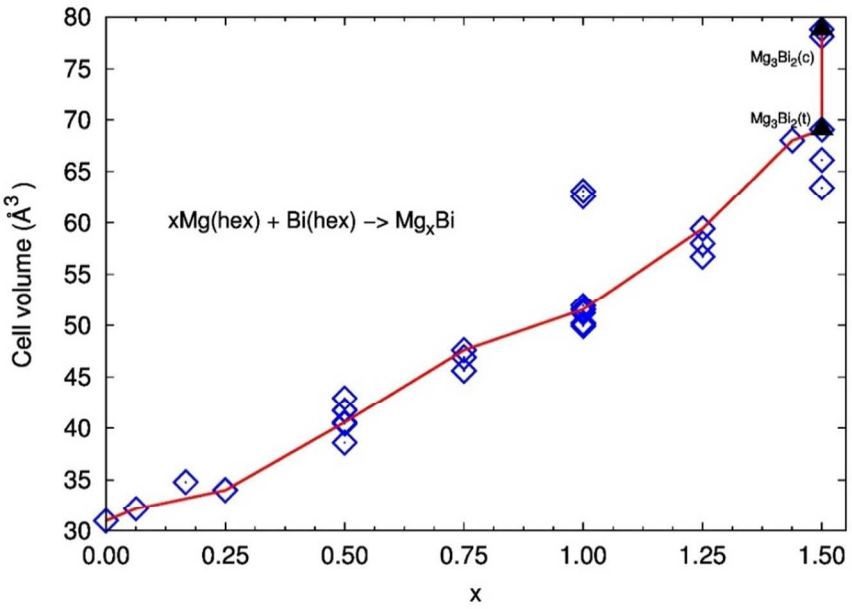


**Figure S6**. The cell volume as a function of magnesium insertion into the hexagonal structure of bismuth, reported per $Mg_xBi$ formula unit. Accordingly, the actual unit cell volumes of the two polymorphs of $Mg_3Bi_2$ (trigonal and cubic) are found by multiplying those of $Mg_{1.5}Bi$ by 2: 138.13 Å$^3$ and 157.61 Å$^3$, respectively.

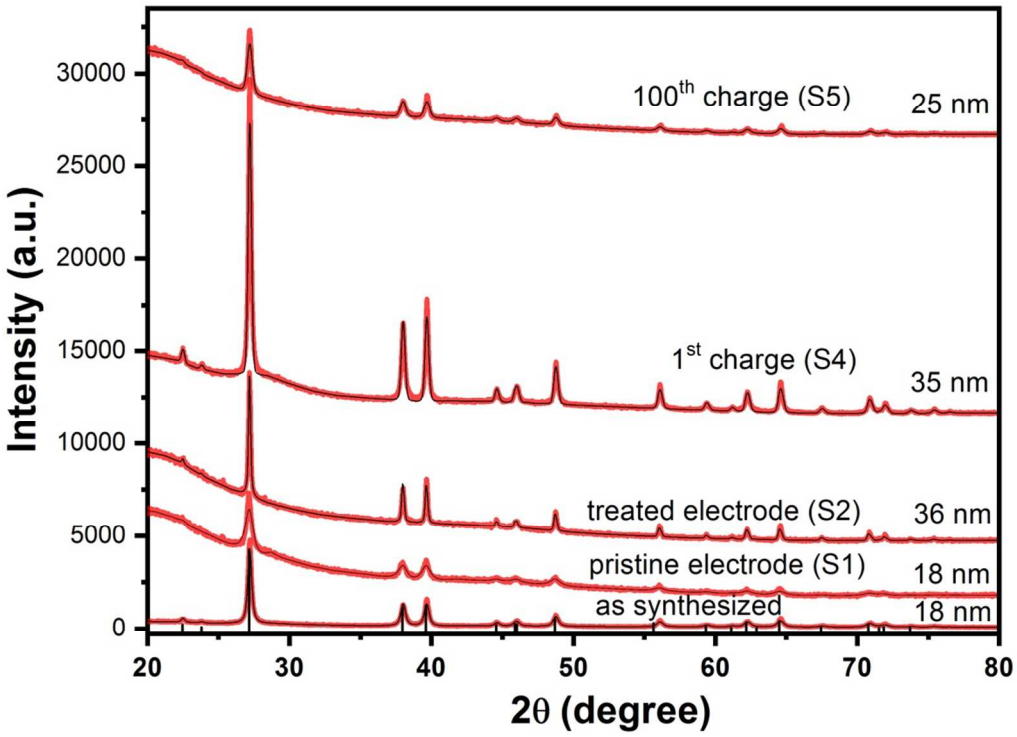


**Figure S7.** Powder XRD patterns of 18 nm Bi NCs after synthesis, electrode preparation (sample S1), electrode hydrazine treatment (sample S2), the first charge (samples S4) and the 100$^{th}$ charge (sample S5). Black vertical lines mark the locations of reflections in the diffraction pattern of bulk Bi; the black curves are the fits obtained by Rietveld refinement. Mean crystallite size may be calculated by the following Scherrer-type formula:

$$D(\text{Å}) = \frac{180K\lambda(\text{Å})}{\pi\sqrt{I_g}}$$

where *Ig* is a parameter obtained by Rietveld refinement and accounts for the isotropic peak broadening due to domain size, K is the shape factor and λ is the wavelength of the X-rays (1.5405 Å).

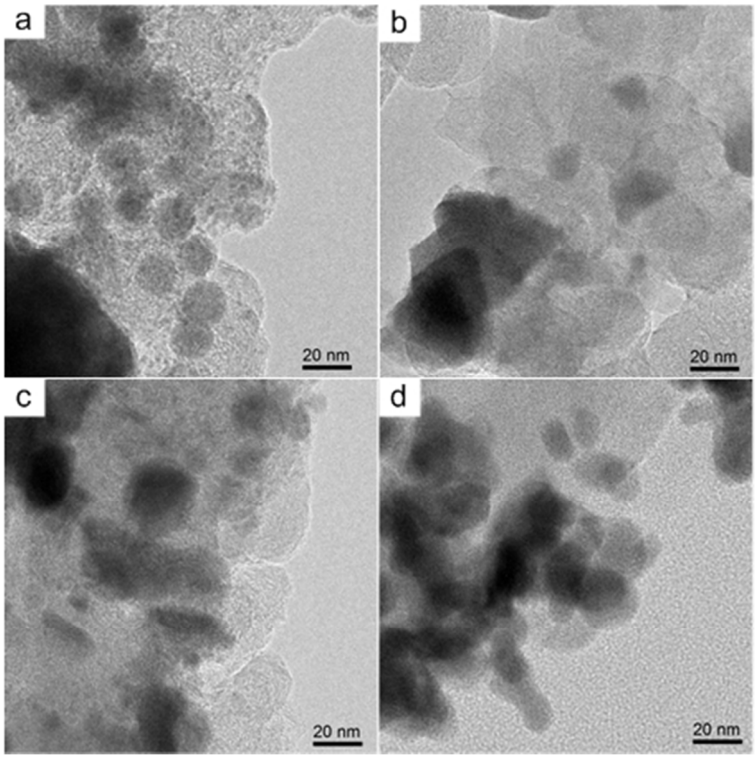


**Figure S8.** TEM images of 18 nm Bi NCs after (a) electrode preparation, (b) hydrazine treatment, (c) the 1st electrochemical discharge, and (d) the 100th electrochemical discharge.

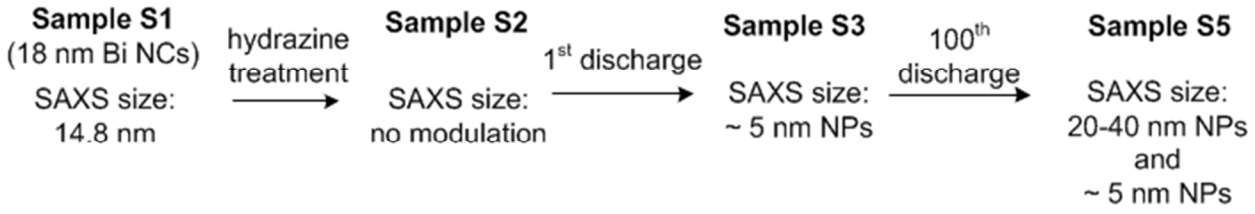


**Figure S9.** Schematic of the size evolution of 18 nm Bi NCs upon electrode preparation, hydrazine treatment, 1st discharge, and 100th discharge, as informed by SAXS analysis.

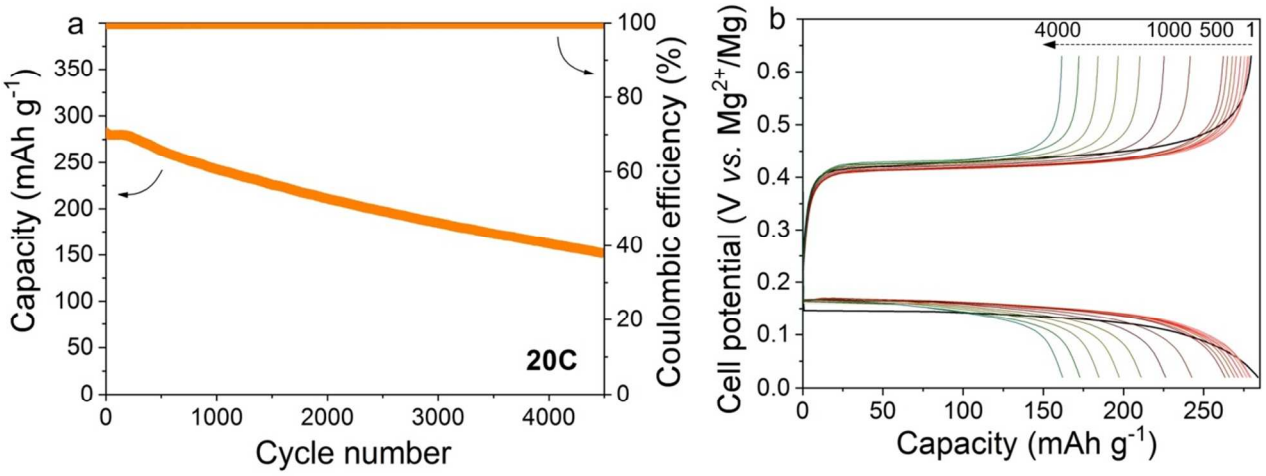


**Figure S10**. Cycling stability (left) and galvanostatic voltage profiles (right) of Mg-ion half-cells using Bi anodes composed of 18 nm Bi NCs at a current rate of 20C (I = 7.7 A $g^{-1}$). Cycle number is indicated in the upper right.

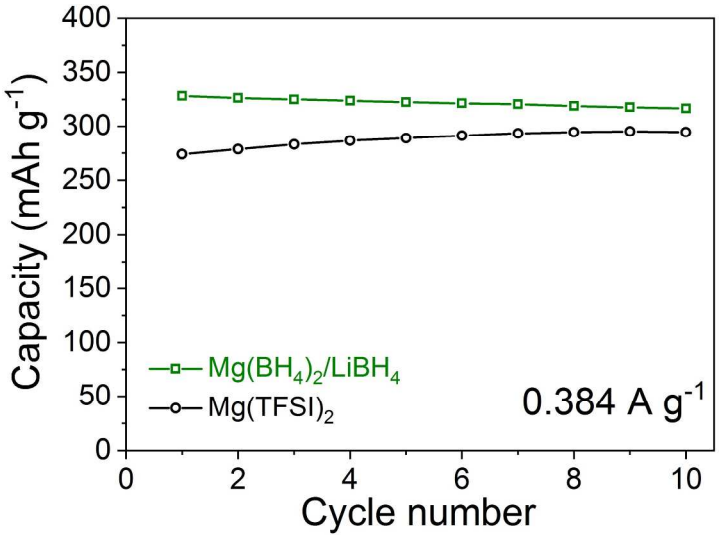


**Figure S11.** Cycling stability of anode-limited full cells (Bi–$Mo_6S_8$) with $Mg(BH_4)_2/LiBH_4$ and $Mg(TFSI)_2$ as the electrolyte, measured at a current rate of 1C (0.384 A $g^{-1}$).

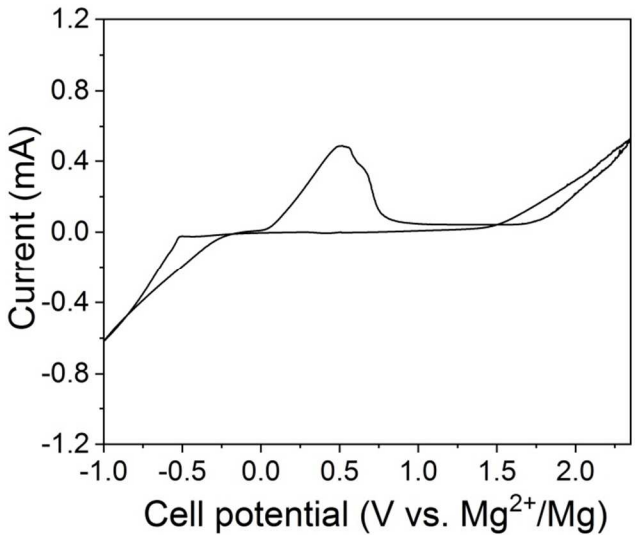


**Figure S12.** Cyclic voltammetry of a Cu current collector measured in $Mg(BH_4)_2/LiBH_4$ electrolyte at a scan rate of 5 mV $s^{-1}$.

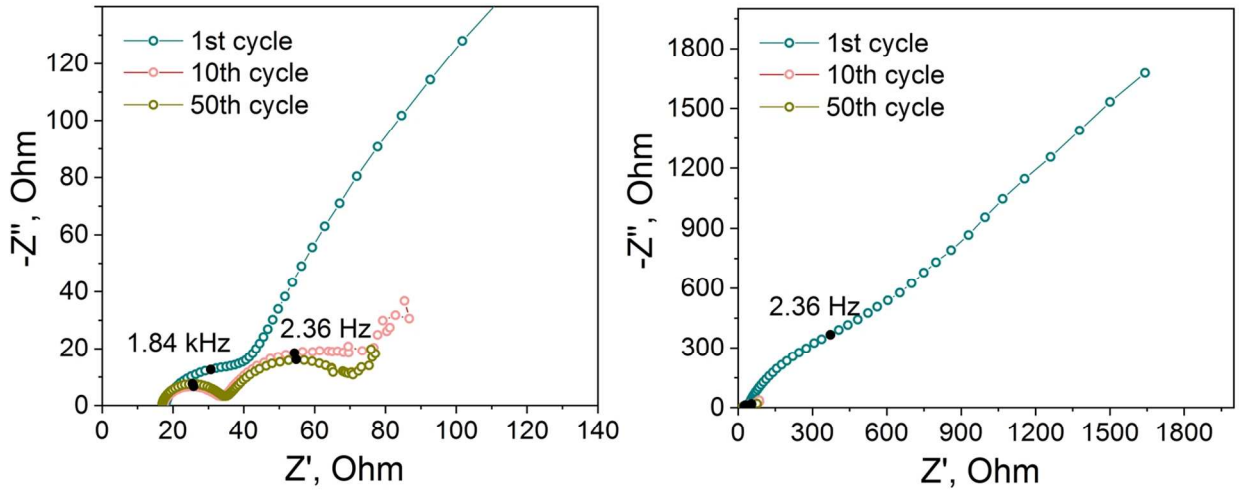


**Figure S13**. Electrochemical impedance analysis of Mg-ion half-cells using Bi anodes composed of 18 nm Bi NCs after the 1st, 10th, and 50th electrochemical cycles. The semicircles in the high and medium-to-low frequency regions represent the resistances associated with a passivation film and the charge-transfer process, respectively. The oblique line in the low-frequency region corresponds to Warburg impedance.

## References

1. Hull, A. W., Crystal Structures of Common Elements. *Phys. Rev.* **1917,** *10*, 661-697.
2. Barrett, C. S., The Structure of Bismuth at Low Temperatures. *Aust. J. Phys.* **1960,** *13*, 208-222.
3. Zintl, E.; Husemann, E., Bindungsart und Gitterbau binaerer Magnesiumverbindungen. (12. Mitteilung ueber Metalle und Legierungen). *Z. Phys. Chem., Abt. B* **1933,** *21*, 138-155.